

1
2
3
4
5
6
7
8
9
10
11
12

A simple, cost-effective, and robust method for rRNA depletion in RNA-sequencing studies

Peter H. Culviner^{1*}, Chantal K. Guegler^{1*}, Michael T. Laub¹⁻³

*These authors contributed equally to this work. See Acknowledgements for explanation of order.

¹Department of Biology, Massachusetts Institute of Technology, Cambridge, MA 02139, USA

²Howard Hughes Medical Institute, Massachusetts Institute of Technology, Cambridge, MA 02139, USA

³Correspondence can be addressed to MTL: laub@mit.edu, 617-324-0418

13 **Abstract**

14 The profiling of gene expression by RNA-sequencing (RNA-seq) has enabled powerful studies of
15 global transcriptional patterns in all organisms, including bacteria. Because the vast majority of
16 RNA in bacteria is ribosomal RNA (rRNA), it is standard practice to deplete the rRNA from a
17 total RNA sample such that the reads in an RNA-seq experiment derive predominantly from
18 mRNA. One of the most commonly used commercial kits for rRNA depletion, the Ribo-Zero kit
19 from Illumina, was recently discontinued. Here, we report the development a simple, cost-
20 effective, and robust method for depleting rRNA that can be easily implemented by any lab or
21 facility. We first developed an algorithm for designing biotinylated oligonucleotides that will
22 hybridize tightly and specifically to the 23S, 16S, and 5S rRNAs from any species of interest.
23 Precipitation of these oligonucleotides bound to rRNA by magnetic streptavidin beads then
24 depletes rRNA from a complex, total RNA sample such that ~75-80% of reads in a typical RNA-
25 seq experiment derive from mRNA. Importantly, we demonstrate a high correlation of RNA
26 abundance or fold-change measurements in RNA-seq experiments between our method and the
27 previously available Ribo-Zero kit. Complete details on the methodology are provided, including
28 open-source software for designing oligonucleotides optimized for any bacterial species or
29 metagenomic sample of interest.

30

31 **Importance**

32 The ability to examine global patterns of gene expression in microbes through RNA-sequencing
33 has fundamentally transformed microbiology. However, RNA-seq depends critically on the
34 removal of ribosomal RNA from total RNA samples. Otherwise, rRNA would comprise upwards
35 of 90% of the reads in a typical RNA-seq experiment, limiting the reads coming from messenger
36 RNA or requiring high total read depth. A commonly used, kit for rRNA subtraction from Illumina
37 was recently discontinued. Here, we report the development of a 'do-it-yourself' kit for rapid, cost-
38 effective, and robust depletion of rRNA from total RNA. We present an algorithm for designing
39 biotinylated oligonucleotides that will hybridize to the rRNAs from a target set of species. We then
40 demonstrate that the designed oligos enable sufficient rRNA depletion to produce RNA-seq data
41 with 75-80% of reads coming from mRNA. The methodology presented should enable RNA-
42 seq studies on any species or metagenomic sample of interest.

43 **Introduction**

44 RNA-sequencing (RNA-seq) is a common and powerful approach for interrogating global patterns
45 of gene expression in all organisms, including bacteria(1–3). In most RNA-seq studies, it is
46 desirable to eliminate rRNAs so that as many reads as possible come from mRNAs(4). For most
47 eukaryotes, the majority of mRNAs are polyadenylated, enabling their selective isolation and
48 subsequent sequencing(5, 6). In contrast, bacteria do not typically poly-adenylate their mRNAs,
49 and rRNA comprises 80% or more of the total RNA harvested from a given sample(7). To enrich
50 for mRNA in RNA-seq samples, a general strategy involves the depletion of rRNAs by subtractive
51 hybridization(8–10). This approach was at the heart of commercially available kits such as Ribo-
52 Zero from Illumina, leading to RNA-seq data in which ~80-90% of the reads map to mRNAs.
53 Despite the popularity and efficacy of Ribo-Zero, this kit was recently discontinued by the
54 manufacturer.

55 Here, we report an easily implemented, scalable, and broadly applicable do-it-yourself (DIY)
56 rRNA depletion kit. Our kit relies on the physical depletion of rRNA from a complex RNA mixture
57 using biotinylated oligonucleotides (oligos) specific to 5S, 16S, and 23S rRNA. We focus
58 primarily on the development of oligos that will enable depletion of rRNA from any one of eight
59 different, commonly studied bacteria. However, we also present an algorithm for customizing the
60 subtractive oligos, and the open-source software developed here can be used to design
61 oligonucleotides for the depletion of rRNA from any user-defined set of species. Our results
62 indicate that the kit we developed enables the facile depletion of rRNA from total RNA samples
63 such that ~70-80% of reads in RNA-seq map to mRNAs. We further demonstrate that our kit
64 produces RNA-seq data showing high correspondence to that produced using Ribo-Zero kit.
65 Additionally, our kit has a reduced cost of only ~\$10 per sample to deplete rRNA from 1 µg of
66 total RNA. We anticipate that this rRNA-depletion strategy will benefit the entire bacterial
67 community by enabling low-cost transcriptomics with a similar workflow to the previously
68 available Ribo-Zero kit.

69 **Results**

70 To efficiently and inexpensively deplete rRNA from total RNA from multiple organisms, we
71 developed an algorithm to design DNA oligonucleotides capable of hybridizing to rRNA from
72 multiple species simultaneously. We reasoned that each rRNA should be bound by multiple oligos

73 across the length of the rRNA, in case a given site is hidden by structure or is not available due to
74 partial fragmentation during RNA extraction or processing. Further, we decided that oligos should
75 be as short as possible to reduce synthesis cost and decrease the likelihood of spurious binding and
76 accidental depletion of mRNA. To find potential binding sites, we aligned the 16S and 23S rRNA
77 sequences from a set of eight commonly studied bacteria, including several major pathogens and
78 model organisms (Figure 1A, S1A). These sequences were divergent enough that we could not
79 design an oligo based on the rRNA sequence of a single species and expect it to bind other the
80 rRNA from other species effectively. Thus, we designed an algorithm to optimize the sequence of
81 oligonucleotides, enabling them to hybridize to rRNA from multiple species. To find these oligos,
82 we focused on ungapped regions of the alignment and chose a large number of sites as candidates
83 (Figure 1B, S1B). For nucleotide positions that were completely conserved among the eight
84 species, the conserved nucleotide was selected. For positions that were only partially conserved, a
85 nucleotide was chosen at random such that it would match a nucleotide found in some but not all
86 of the rRNAs.

87 We then performed an iterative process to sample alternate sequences and binding locations for
88 each oligo, while biasing the selection toward sequences that tightly bind rRNA from the eight
89 species we had selected. To do this, for each oligo we generated *in silico* a set of mutated
90 oligonucleotides that varied from the original sequence by either extending, shrinking, or shifting
91 the binding site, or by mutating a single nucleotide of the oligonucleotide to match a different
92 species' rRNA. From this set of mutated oligonucleotides, the algorithm effectively replaced each
93 old oligonucleotide with a new one, favoring those close to a target minimum T_m of 62.5 °C. This
94 T_m was chosen to achieve tight binding across all species while preventing selection of excessively
95 long oligonucleotides. With more cycles of optimization, the average minimum T_m approaches the
96 target T_m (Figure 1C, S1C). Notably, many oligonucleotides, particularly those with poorly
97 conserved start locations, were not able to reach the target T_m , though the number that did increased
98 with additional cycles (Figure 1D, S1D). After 15-20 cycles, the oligonucleotides had converged
99 on highly conserved regions of the rRNAs (Figure 1B-D, S1B-D). After 100 cycles of
100 optimization, we selected 8 and 9 non-overlapping oligonucleotides for the 16S and 23S rRNA,
101 respectively, with an average length of 30 nucleotides. These 17 oligos are predicted to hybridize
102 to rRNA from all eight species included in the initial design. Although the T_m for individual oligos
103 varies across species, the mean T_m for the oligo set as a whole was similar (Figure 1E, S1E).

104 We also applied our algorithm to the 5S rRNA from the 8 species considered. However, because
105 the 5S rRNA is both shorter and more poorly conserved than 16S and 23S rRNA, we were unable
106 to find oligos that are predicted to effectively hybridize to the 5S rRNA from all eight species.
107 Therefore, we ran the algorithm against individual 5S rRNAs and hand-selected two oligos specific
108 to the 5S from each species. In addition, we found that the algorithm was unable to find oligos
109 mapping near the 5'- and 3'-ends of the 23S due to its low conservation among species. To improve
110 binding to these regions, we also identified two oligos that were specific to either Gram-positive
111 or Gram-negative members of our target set of species. Thus, our final set of depletion oligos for
112 a given organism includes 21 total oligos: 17 common oligos targeting 16S and 23S rRNA, 2 oligos
113 that target 23S rRNA in a Gram positive- or Gram-negative-specific manner, and 2 species-
114 specific 5S targeting oligos (Table S1; oligos each contain a 5'-biotin modification).

115 We then sought to determine whether our oligo libraries could effectively deplete bacterial rRNA.
116 To deplete rRNAs from a total RNA sample, we incubated biotinylated versions of the 21 designed
117 oligos with total RNA. Samples were then combined with magnetic streptavidin beads to
118 precipitate the oligos bound to rRNAs, followed by isolation of the supernatant, which should be
119 heavily enriched for mRNA (Figure 2A). We extracted total RNA from exponentially growing
120 cultures of common lab strains of *E. coli*, *B. subtilis*, and *C. crescentus* and performed a single
121 round of rRNA depletion. For all three species, incubation with the 21 depletion oligos
122 substantially decreased the intensity of rRNA signal on a polyacrylamide gel, while tRNA and
123 ncRNA were generally unaffected (Figure 2B). Moreover, this depletion was modular, as
124 incubation of *E. coli* total RNA with probes targeting only 16S, 23S, or 5S rRNA resulted in
125 selective depletion of the band corresponding to a given targeted rRNA (Figure 2B, left).

126 To quantify how well our method depleted rRNA, we performed RNA-seq on the three RNA
127 samples pre- and post-rRNA depletion for *E. coli*, *B. subtilis*, and *C. crescentus*. We then
128 calculated the fraction of reads mapping to rRNA loci in each case (Figure 2C). The fraction
129 mapping to rRNA decreased following depletion from >95% to 13%, 6%, and 22%, respectively.
130 To determine whether there was any bias for depletion of certain regions of the rRNAs, we
131 compared read counts at each nucleotide position pre- and post-depletion in each *E. coli* rRNA
132 (Figure 2D). For the 16S, 23S, and 5S rRNAs, read density was relatively uniform but lower,
133 following depletion, indicating that no particular region of the rRNAs (e.g. regions prone to high

134 structure or partial degradation, preventing effective depletion) was over-represented in our rRNA
135 reads.

136 Many RNA-seq studies are aimed at detecting significant differences in the expression of mRNA
137 in different strains or across different perturbations. To ensure that our depletion technique did not
138 affect the measurement of expression changes (e.g. through unintended depletion of particular
139 mRNAs), we treated *E. coli* cells with either rifampicin or chloramphenicol for 5 minutes and
140 compared fold changes measured from libraries generated using our depletion strategy to those
141 generated using the previously available commercial kit Ribo-Zero (Illumina). For each depletion
142 method, we calculated the \log_2 fold-change in read counts in coding regions following antibiotic
143 treatment compared to a negative control (Figure 3A-B). For both rifampicin and chloramphenicol
144 treatment, the correlation in \log_2 fold-change per coding region between the two rRNA depletion
145 strategies was high ($R^2 = 0.98$ and 0.97 for rifampicin and chloramphenicol, respectively) across
146 a wide range of changes in gene expression. These results indicate that our method should provide
147 similar results to the Ribo-Zero kit for studies measuring changes in gene expression.

148 Importantly, we also determined if our kit differentially depleted particular mRNAs compared to
149 the Ribo-Zero kit. To do this, we directly compared the RPKM (reads per kilobase per million)
150 values for well-expressed coding regions from a library prepared using our depletion strategy and
151 one prepared using Ribo-Zero (Figure 3C). Overall, there was a high correlation between the two
152 depletion methods ($R^2 = 0.89$). However, there were a few outliers. We first identified genes more
153 than two standard deviations away from a log-linear fit of RPKM in a comparison of RNA-seq
154 data generated using our method and Ribo-Zero (Figure S2A). To ensure that fold-change in
155 expression could also be accurately calculated for these outliers, we returned to the data generated
156 following antibiotic treatment (Figure 3A-B). For the outlier genes, the change in expression
157 following treatment with rifampicin or chloramphenicol was still highly correlated (Figure S2B-
158 C; $R^2 = 0.95$ and 0.90 , respectively). For a more stringent cut-off, we also hand-selected 11 of the
159 most highly expressed outliers that were more significantly depleted by our method than Ribo-
160 Zero (Figure S2D). Again, the changes in expression calculated following treatment with
161 rifampicin or chloramphenicol were highly correlated (Figure S2E-F; $R^2 = 0.96$ and 0.89 for
162 rifampicin and chloramphenicol, respectively). Thus, results obtained based on our
163 oligonucleotide hybridization approach are highly comparable to those generated with the
164 previously-available Ribo-Zero kit.

165 Finally, we compared the RPKM values for well-expressed coding regions between libraries
166 prepared using our depletion strategy and libraries from total RNA (no rRNA depletion) from *E.*
167 *coli*, *B. subtilis*, and *C. crescentus* (Figure S3A). Depleted libraries for each species showed similar
168 correlations of $R^2 = 0.76$, 0.71 , and 0.66 for *E. coli*, *B. subtilis*, and *C. crescentus*, respectively
169 (Figure S3A). Though this analysis is complicated by the relatively few reads mapping to mRNA
170 in undepleted samples (Figure 2C), these results confirm that our method is an effective strategy
171 for depleting rRNAs while maintaining transcriptome composition across multiple species. Taken
172 all together, we conclude that our DIY method provides a broadly applicable, customizable, and
173 cost-effective technique for determining changes in bacterial gene expression patterns in a wide
174 range of organisms and experimental contexts.

175 Discussion

176 We have developed a simple, fast, easy-to-implement, and cost-effective method for efficiently
177 depleting rRNA from complex, total RNA samples. For three different species, *E. coli*, *B. subtilis*,
178 and *C. crescentus*, we demonstrated robust depletion of 23S, 16S, and 5S rRNAs in a single step
179 such that ~70-90% of reads in RNA-seq arise from non-rRNA sources. This level of mRNA
180 enrichment is sufficient for most RNA-seq studies. Our method showed relatively uniform
181 depletion of rRNAs and minimal, unwanted 'off-targeting' of mRNAs. Additionally, expression
182 changes measured using our method correlated very strongly ($R^2 = 0.98$, 0.97 ; Figure 3A-B) to
183 those measured using the previously available Ribo-Zero kit. This strong correlation both validates
184 our method and ensures that data generated via either method can be safely compared or combined.

185 Another method has recently been developed as an alternative to the discontinued Ribo-Zero
186 kit(11). This method is based on hybridization of DNA oligonucleotides to rRNAs followed by
187 digestion with RNase H, which recognizes DNA:RNA hybrids. This method also enabled robust
188 rRNA depletion, although a direct comparison of RNA-seq counts per gene generated using this
189 method and Ribo-Zero was not reported. Additionally, this alternative method requires extended
190 (~60 min) incubations with an RNase, albeit one that should be specific to DNA-RNA hybrids,
191 whereas ours involves only hybridization and a precipitation step.

192 The set of biotinylated oligonucleotides tested here were designed to deplete the rRNA from a set
193 of 8 selected organisms. These organisms span a large phylogenetic range so these
194 oligonucleotides are likely broadly applicable to different bacterial species or even metagenomic

195 samples. However, the set of oligonucleotides can also be easily optimized for a different species
196 or set of species using the open-source software developed here and available on Github. As noted,
197 because the 5S rRNA is shorter and less conserved, probes specific to the 5S from a given species
198 must typically be designed. However, the 5S rRNA does not yield nearly as many reads in RNA-
199 seq data for a total RNA sample and may not require depletion for all studies.

200 In sum, the rRNA depletion methodology developed here should facilitate RNA-seq studies for
201 any bacterium of interest. Notably, our method is also substantially cheaper than the Ribo-Zero
202 kit. The cost of our method is ~\$10 per reaction to deplete 1 μ g of total RNA (see Methods)
203 compared to ~\$80 per reaction for Ribo-Zero. The cost for our approach stems primarily from the
204 magnetic streptavidin beads used to precipitate the biotinylated oligonucleotides bound to rRNA.
205 Further optimization of the method reported here could likely reduce the cost further and possibly
206 improve the extent of rRNA depletion. Nevertheless, as currently implemented, our method should
207 enable the community to perform relatively easy, cost-effective, robust rRNA depletion, thereby
208 facilitating RNA-seq studies.

209

210

211 **Materials and Methods**

212 **Oligonucleotide algorithm**

213 The algorithm was initialized with 500 and 1000 oligos of length 15 to 24 nucleotides for the 16S
214 and 23S rRNA, respectively. Oligos were randomly positioned at non-gapped locations of the
215 alignment of the 8 species we selected. Sequences were chosen by randomly selecting a nucleotide
216 matching one or more species at each position. Sequences were then optimized to achieve the
217 target predicted T_m of 62.5°C. T_m calculations were conducted using the MeltingTemp module in
218 the biopython library. We used the default nearest-neighbor calculation table for RNA-DNA
219 hybrids(12). Notably, this model does not allow prediction of T_m for some sequences with multiple
220 sequential mismatches; as such, many oligos begin the optimization with undefined T_m .

221 Optimization was conducted by sequential rounds of ‘mutation’ on each oligo. Allowed mutations
222 included moving the probe from 1-4 bases, shrinking the probe from 1-4 bases (on either end),
223 extending the probe from 1-4 bases (on either end), or swapping the sequence of the oligo at one
224 position to a nucleotide matching a different aligned rRNA. In each round of mutation, the starting
225 oligo was mutated 25 times. From this set of mutated oligos, an oligo close to the target T_m was
226 chosen probabilistically (probabilities were determined by a normal distribution centered at 62.5°C
227 with a standard deviation of 2°C). This probabilistic selection, coupled with the large number of
228 oligos initialized, enables oligos to sample the possible binding locations without greedily
229 descending on the first possible binding site they discover. Each oligo was mutated for 100 cycles
230 before oligos binding to a number of sites across the 16S and 23S were selected.

231 To enable better binding of the more variable 23S 5'- and 3'-ends, we split the organisms into two
232 groups (Ec, Pa, Cc, Rp and Ms, Mtb, Bs, Sa) and re-ran the optimization algorithm as above. For
233 each of these groups, we selected 2 additional oligos matching the 5'- and 3'-ends of the 23S.

234 **Data and code availability**

235 The code used to generate the oligonucleotides is available for download at
236 <https://github.com/peterculviner/ribodeplete>. The raw and processed sequencing data is available
237 on GEO (GSE142656).

238 **Bacterial strains and culture condition**

239 *E. coli* MG1655 was grown to mid-log phase at 37 °C in LB medium or M9 medium supplemented
240 with 0.1% casamino acids, 0.4% glucose, 2 mM MgSO₄, and 0.1 mM CaCl₂. *C. crescentus*

241 CB15N/NA1000 was grown to mid-log phase in PYE medium at 30 °C. *B. subtilis* 168 was grown
242 to mid-log phase at 37 °C in LB medium. For quantifying changes in expression from antibiotic
243 treatment, cells were harvested 5 minutes after adding chloramphenicol or rifampicin at 50 µg/mL
244 or 25 µg/mL, respectively.

245 **RNA extraction**

246 *E. coli* RNA was harvested by mixing 1 mL of cells with 110 µL of ice-cold stop solution (95%
247 ethanol and 5% acid-buffered phenol) and spinning in a table-top centrifuge for 30 s at 13000 rpm.
248 *C. crescentus* RNA was harvested by spinning down 2 mL of cells in a table-top centrifuge for 30
249 s at 13000 rpm. After removing the supernatant, pellets were flash-frozen and stored at -80 °C until
250 sample collection was complete. To extract RNA, TRIzol (Invitrogen) was heated to 65 °C and
251 added to each cell pellet. The mixtures were then shaken at 65 °C for 10 min at 2000 rpm in a
252 thermomixer and flash-frozen at -80 °C for at least 10 min. Pellets were thawed at room
253 temperature and spun at top speed in a benchtop centrifuge at 4 °C for 5 min. The supernatant was
254 added to 400 µL of 100% ethanol and passed through a DirectZol spin column (Zymo). Columns
255 were washed twice with RNA PreWash buffer (Zymo) and once with RNA Wash buffer (Zymo),
256 and RNA was eluted in 90 µL DEPC H₂O. To remove genomic DNA, RNA was then treated with
257 4 µL of Turbo DNase I (Invitrogen) in 100 µL supplemented 10x Turbo DNase I buffer for 40 min
258 at 37 °C. RNA was then diluted with 100 µL DEPC H₂O, extracted with 200 µL buffered acid
259 phenol-chloroform, and ethanol precipitated at -80 °C for 4 hr with 20 µL of 3 M NaOAc, 2 µL
260 GlycoBlue (Invitrogen), and 600 µL ice-cold ethanol. Samples were centrifuged at 4 °C for 30 min
261 at 21000 x g to pellet RNA, then washed twice with 500 µL of ice-cold 70% ethanol, followed by
262 centrifugation at 4 °C for 5 min. RNA pellets were then air-dried and resuspended in DEPC H₂O.
263 RNA yield was quantified by a NanoDrop spectrophotometer, and RNA integrity was verified by
264 running 50 ng of total RNA on a Novex 6% TBE-urea polyacrylamide gel (Invitrogen).

265 *B. subtilis* total RNA was harvested by mixing 5 mL of cell culture with 5 mL of cold (-30 °C)
266 methanol and spinning down at 5000 rpm for 10 min. After removing the supernatant, pellets were
267 frozen at -80 °C. To lyse cells, pellets were vortexed in 100 µL lysozyme (10 mg/mL) in TE (10
268 mM Tris-HCl and 1 mM EDTA) at pH = 8.0 and incubated for 5 min at 37 °C. Lysates were
269 cleared by adding 350 µL Buffer RLT (Qiagen) in 1% beta-mercaptoethanol and vortexing.
270 Lysates were then mixed with 250 µL ethanol, vortexed, and passed through an RNeasy mini spin
271 column (Qiagen). Columns were washed with 350 µL Buffer RW1 (Qiagen). To remove genomic

272 DNA, 40 μ L of DNaseI in Buffer RDD (Qiagen) was applied to each column, and columns were
273 incubated at room temperature for 15 min. Columns were then washed once with 350 μ L Buffer
274 RW1 (Qiagen) and twice with Buffer RPE (Qiagen), and RNA was eluted in 30 μ L DEPC H₂O.
275 RNA yield was quantified by a NanoDrop spectrophotometer, and RNA integrity was verified by
276 running 50 ng of total RNA on a Novex 6% TBE-urea polyacrylamide gel (Invitrogen).

277 **rRNA depletion, DIY method**

278 Biotinylated oligos were selected using our algorithm, synthesized by IDT, and resuspended to
279 100 μ M in Buffer TE (Qiagen). An undiluted oligo mix for each organism was created by mixing
280 equal volumes of all 16S and 23S primers, as well as double volumes of 5S primers. This undiluted
281 mix was then diluted based on the amount of total RNA added to the depletion reaction, using a
282 custom bead calculator (available with code at <https://github.com/peterculviner/ribodeplete>).

283 Dynabeads MyOne Streptavidin C1 beads (ThermoFisher) were washed three times in an equal
284 volume of 1x B&W buffer (5 mM Tris HCl pH = 7.0, 5 mM Tris HCl pH = 7.0, 500 μ M EDTA,
285 1 M NaCl) and then resuspended in 30 μ L of 2x B&W buffer (10 mM Tris HCl pH = 7.0, 10 mM
286 Tris HCl pH = 7.0, 1 mM EDTA, 2 M NaCl). To prevent RNase contamination, 1 μ L of
287 SUPERase-In RNase Inhibitor (ThermoFisher) was added to the beads. The beads were then
288 incubated at room temperature until probe annealing (below) was complete.

289 To anneal biotinylated probes to rRNA, 2-3 μ g total RNA, 20x SSC, 30 mM EDTA, water, and
290 the diluted probe mix were mixed on ice in the calculated quantities. The mixtures were incubated
291 in a thermocycler at 70 $^{\circ}$ C for 5 min, followed by a slow ramp down to 25 $^{\circ}$ C at a rate of 1 $^{\circ}$ C per
292 30 sec. To pull down biotinylated probes bound to rRNA, annealing reactions were then added
293 directly to beads in 2x B&W buffer, mixed by pipetting and vortexing at medium speed, and
294 incubated for 5 min at room temperature. Reactions were then vortexed on medium speed and
295 incubated at 50 $^{\circ}$ C for 5 min, and then placed directly on a magnetic rack to separate beads from
296 the remaining total RNA. The supernatant was pipetted away from the beads, placed on ice, and
297 diluted to 200 μ L in DEPC H₂O. RNA was then ethanol precipitated at -20 $^{\circ}$ C for at least 1 hour
298 with 20 μ L of 3 M NaOAc, 2 μ L GlycoBlue (Invitrogen), and 600 μ L ice-cold ethanol. Samples
299 were centrifuged at 4 $^{\circ}$ C for 30 min at 21000 x g to pellet RNA, then washed twice with 500 μ L
300 of ice-cold 70% ethanol, followed by centrifugation at 4 $^{\circ}$ C for 5 min. RNA pellets were then air-
301 dried and resuspended in 10 μ L DEPC H₂O. RNA yield was quantified by a NanoDrop

302 spectrophotometer, and the efficiency of rRNA depletion was verified by running 50 ng of total
303 RNA on a Novex 6% TBE-urea polyacrylamide gel (Invitrogen).

304 **Optimization of rRNA depletion**

305 In the process of generating our depletion protocol, we tried multiple ratios of streptavidin-coated
306 beads to biotinylated oligos and biotinylated oligos to total RNA. We found that rRNA was
307 depleted robustly across a range of ratios. However, it was critical to have a significant excess of
308 streptavidin-coated beads over biotinylated oligos, as oligos that do not successfully capture rRNA
309 may bind streptavidin more rapidly, thus out-competing bound rRNA-bound oligos and reducing
310 rRNA capture efficiency. We selected our final ratios to achieve reliable depletion of rRNA at a
311 low per-reaction cost.

312 **Cost calculation**

313 The majority of reagents are common laboratory supplies for labs that work with RNA. To
314 maintain the optimized ratio between streptavidin beads, biotinylated oligos, and rRNA, more
315 oligos and beads must be used to deplete more total RNA. Considering the input, the cost per
316 reaction is approximately \$10, \$19, or \$28 for 1, 2 or 3 μ g of RNA, respectively. The majority of
317 the cost per reaction arises from streptavidin-coated magnetic beads; cost could likely be further
318 decreased by using cheaper streptavidin-coated beads or decreasing the quantity of beads used (see
319 above). The up-front cost of purchasing oligos (IDT) is approximately \$1000 for large scale
320 synthesis or \$500 for smaller scale synthesis (available for sets of oligos >24). However, a single
321 oligo synthesis order is adequate for hundreds of depletion reactions.

322 **RNA-seq library preparation**

323 Libraries were generated as previously with a few modifications described below(13). The library
324 generation protocol was a modified version of the paired-end strand-specific dUTP method using
325 random hexamer priming. For libraries without rRNA removal, 500 ng of total RNA was used in
326 the fragmentation step. For libraries with rRNA removal, 2-3 μ g of input RNA was used in the
327 rRNA removal step.

328 **rRNA depletion by Ribo-Zero**

329 rRNA depletion via Ribo-Zero treatment (Illumina) was conducted as described previously(13).
330 Briefly, provided magnetic beads were prepared individually by adding 225 μ L of beads to a
331 1.5 mL tube, left to stand on a magnetic rack for 1 minute, washed twice with 225 μ L of water,

332 and resuspended in 65 μL of provided resuspension solution with 1 μL of provided RNase
333 inhibitor. Samples were prepared using provided reagents with 4 μL of reaction buffer, 2-3 μg of
334 total RNA, 10 μL of rRNA removal solution in a total reaction volume of 40 μL . Samples were
335 incubated at 68 $^{\circ}\text{C}$ for 10 minutes and at room temperature for 5 minutes. Samples were added
336 directly to the resuspended magnetic beads, mixed by pipetting, incubated for 5 minutes at room
337 temperature, and then incubated for 5 minutes at 50 $^{\circ}\text{C}$. After incubation, samples were placed on
338 magnetic rack and the supernatant was transferred to a new tube, discarding the beads. Samples
339 were ethanol precipitated as above with a 1 hour incubation at -20°C and resuspended in 9 μL of
340 water.

341 **Fragmentation**

342 RNA libraries were fragmented by adding 1 μL of 10x fragmentation buffer (Invitrogen) to 9 μL
343 of input RNA in DEPC H_2O and heating at 70 $^{\circ}\text{C}$ for 8 min. Fragmentation reactions were stopped
344 by immediately placing on ice and adding 1 μL of stop solution (Invitrogen). Reactions were
345 diluted to 20 μL in DEPC H_2O , and RNA was ethanol precipitated at -20°C for at least 1 hour
346 with 2 μL of 3 M NaOAc, 2 μL GlycoBlue (Invitrogen), and 60 μL ice-cold ethanol. Samples were
347 centrifuged at 4 $^{\circ}\text{C}$ for 30 min at 21000 x g to pellet RNA, then washed with 200 μL of ice-cold
348 70% ethanol, followed by centrifugation at 4 $^{\circ}\text{C}$ for 5 min. RNA pellets were then air-dried and
349 resuspended in 6 μL DEPC H_2O .

350 **cDNA synthesis**

351 1 μL of random primers at 3 $\mu\text{g}/\mu\text{L}$ (Invitrogen) were added to fragmented RNA, and the mixture
352 was heated at 65 $^{\circ}\text{C}$ for 5 min and placed on ice for 1 min. To conduct first strand synthesis, 4 μL
353 of first strand synthesis buffer (Invitrogen), 2 μL of 100 mM DTT, 1 μL of 10 mM dNTPs, 1 μL
354 of SUPERase-In (Invitrogen), and 4 μL of DEPC H_2O were added to each reaction. Reaction
355 mixtures incubated at room temperature for 2 minutes, followed by addition of 1 μL of Superscript
356 III. Reactions were then placed in a thermocycler for the following program: 25 $^{\circ}\text{C}$ for 10 min, 50
357 $^{\circ}\text{C}$ for 1 hr, and 70 $^{\circ}\text{C}$ for 15 min. To extract cDNA, reactions were diluted to 200 μL in DEPC
358 H_2O , then vortexed with 200 μL of neutral phenol-chloroform isoamyl alcohol. Following
359 centrifugation, the aqueous layer was extracted, and cDNA was ethanol precipitated at -20°C for
360 at least 1 hour with 18.5 μL of 3 M NaOAc, 2 μL GlycoBlue (Invitrogen), and 600 μL ice-cold
361 ethanol. Samples were centrifuged at 4 $^{\circ}\text{C}$ for 30 min at 21000 x g to pellet cDNA, then washed
362 twice with 500 μL of ice-cold 70% ethanol, followed by centrifugation at 4 $^{\circ}\text{C}$ for 5 min. Pellets

363 were then air-dried and resuspended in 104 μL DEPC H_2O . Second strand synthesis was conducted
364 by adding 30 μL of second strand synthesis buffer (Invitrogen), 4 μL of 10 mM dNTPs (with dUTP
365 instead of dTTP), 4 μL of first strand synthesis buffer (Invitrogen), and 2 μL of 100 mM DTT to
366 each sample, followed by incubation on ice for 5 min. To initiate second strand synthesis, 1 μL of
367 RNase H (NEB), 1 μL of *E. coli* DNA ligase (NEB), and 4 μL of *E. coli* DNA polymerase I (NEB)
368 were added to each sample. Reactions were then incubated at 16 $^\circ\text{C}$ for 2.5 hr.

369 **End-repair and adaptor ligation**

370 Cleanup for second strand synthesis and all subsequent steps was conducted using Agencourt
371 AMPure XP magnetic beads (Beckman Coulter), and beads were left in the reaction to be reused
372 for subsequent cleanup steps. For each sample, 100 μL of beads were added to 1.5 mL tubes and
373 placed on a magnetic rack. The supernatant was removed and replaced with 450 μL of 20% (w/v)
374 PEG 8000 in 2.5 M NaCl. Second strand synthesis reactions were then added directly to
375 resuspended beads, mixed by pipetting and vortexing, and incubated at room temperature for 5
376 min. Samples were then placed on a magnetic rack for \sim 10 min, or until the solution was clear,
377 and the supernatant was removed. Beads were then washed twice in 500 μL of 80% ethanol, dried,
378 and resuspended in 50 μL of elution buffer (Qiagen). End repair reactions were conducted by
379 adding 10 μL of 10x T4 DNA ligase buffer (NEB), 4 μL of 10 mM dNTPs, 5 μL of T4 DNA
380 polymerase (NEB), 1 μL of Klenow DNA polymerase (NEB), 5 μL of T4 polynucleotide kinase
381 (NEB), and 25 μL of DEPC H_2O and incubating at 25 $^\circ\text{C}$ for 30 min. To clean up the reactions,
382 300 μL of 20% (w/v) PEG 8000 in 2.5 M NaCl was mixed with each reaction by pipetting and
383 vortexing. Samples were then incubated at room temperature for 5 min, and then placed on a
384 magnetic rack for \sim 5 min. The supernatant was removed, and the beads were then washed twice
385 in 500 μL of 80% ethanol, dried, and resuspended in 32 μL of elution buffer (Qiagen). 3'-
386 adenylation reactions were conducted by adding 5 μL of NEB buffer 2 (NEB), 1 μL 10 mM dATP,
387 3 μL Klenow fragment (3' \rightarrow 5' exo-) (NEB), and 9 μL of DEPC H_2O to each reaction and
388 incubating at 37 $^\circ\text{C}$ for 30 min. To clean up the reactions, 150 μL of 20% (w/v) PEG 8000 in 2.5
389 M NaCl was mixed with each reaction by pipetting and vortexing. Samples were then incubated
390 at room temperature for 5 min, and then placed on a magnetic rack for \sim 5 min. The supernatant
391 was removed, and the beads were then washed twice in 500 μL of 80% ethanol, dried, and
392 resuspended in 20 μL of elution buffer (Qiagen). To elute DNA from the beads, reactions were
393 incubated at room temperature for 5 min. Tubes were then returned to the magnetic rack and

394 incubated for 1-2 min to allow the solution to clear, and then half of the supernatant (10 μ L) was
395 removed and stored at -20 °C in case of downstream failure. To ligate adaptors to DNA, 1 μ L of 5
396 μ M annealed adaptors and 10 μ L of Blunt/TA ligase master mix (NEB) was added to each reaction,
397 and reactions were incubated at 25 °C for 20 min. Annealed adaptor mix was made by mixing
398 25 μ L of a 200 μ M solution of each paired-end adaptor together, heating to 90°C for 2 minutes,
399 cooling at 2°C/minute for 30 minutes on a thermocycler, placing on ice, adding 50 μ L of water,
400 and storing aliquots at -20°C. To clean up ligation reactions, 60 μ L of 20% (w/v) PEG 8000 in
401 2.5 M NaCl was mixed with each reaction by pipetting and vortexing, and reactions were incubated
402 at room temperature for 5 min. Reactions were then placed on a magnetic rack for ~10 min, until
403 solutions were clear, and the supernatant was removed. The beads were then washed twice in 500
404 μ L of 80% ethanol, dried, and resuspended in 19 μ L of 10 mM Tris-HCl (pH = 8) and 0.1 mM
405 EDTA. Reactions were then incubated at room temperature for 5 min to completely elute DNA.
406 Tubes were then returned to the magnetic rack and incubated for 1-2 min to allow the solution to
407 clear, and then the supernatant was removed and moved to a new tube and the beads discarded. To
408 digest the dUTP-containing second strand, 1 μ L of USER enzyme (NEB) was added to 19 μ L of
409 eluted DNA and incubated at 37 °C for 15 min, followed by heat-inactivation at 95 °C for 5 min.

410 **Library amplification**

411 PCR reactions were prepared by mixing 10 μ L of library template (diluted if too concentrated), 2
412 μ L of 25 μ M global primer, 2 μ L of 25 μ M barcoded primer, 11 μ L of H₂O, and 25 μ L of 2x
413 KAPA HiFi HotStart ReadyMix (Roche). Reactions were then cycled through the following
414 thermocycler protocol: 98 °C/45 s, 98 °C/15 s, 60 °C/30 s, 72 °C/30 s, 72 °C/1 min. Steps 2-4 were
415 repeated for 9-12 cycles, depending on the results of 10 μ L optimization reactions. Following
416 amplification, PCR reactions were run on an 8% TBE polyacrylamide gel (Invitrogen) for 30 min
417 at 180 V, and the region from 200 to 350 bp was excised, crushed, soaked in 500 μ L 10 mM Tris
418 pH = 8.0, and frozen at -20 °C for at least 15 min. To elute DNA from the gel, reactions were
419 shaken at 2000 rpm for 10 min at 70 °C in a thermomixer, followed by 1 hr at 37 °C. Reactions
420 were then spun through a Spin-X 0.22 μ m cellulose acetate column (Costar) and transferred to a
421 new tube. Libraries were isopropanol precipitated by adding 32 μ L 5 M NaCl, 2 μ L GlycoBlue
422 (Invitrogen), and 550 μ L 100% isopropanol and incubating at -20 °C for at least 1 hr. Samples
423 were then centrifuged at 4 °C for 30 min at 21000 x g to pellet DNA, then washed with 1 mL of
424 ice-cold 70% ethanol, followed by centrifugation at 4 °C for 5 min. DNA pellets were then air-

425 dried and resuspended in 11 μ L H₂O. Paired-end sequencing of amplified libraries was then
426 performed on an Illumina NextSeq500, and single-end sequencing on an Illumina MiSeq.

427 **RNA-sequencing read mapping and normalization.**

428 FASTQ files for each barcode were mapped to the *E. coli* MG1655 genome (NC_000913.2), the
429 *B. subtilis* 168 genome (NC_000964.3), or the *C. crescentus* NA1000 genome (NC_011916.1)
430 using bowtie2 (version 2.1.0) with the following arguments: -D 20 -R 3 -N 0 -L 20 -i S,1,0.50.
431 The samtools (version 0.1.19) suite was used via the pysam library (version 0.9.1.4) for
432 interconversion of BAM and SAM file formats and conducting indexing. Gene names and coding
433 region positions were extracted from NCBI annotations.

434 **Single-end sequencing**

435 For all analyses except that of fragment density across *E. coli* rRNA loci, one count was added to
436 the middle of each read. All reads mapping to a given coding region were then summed and
437 normalized by reads per kilobase of transcript per million (RPKM). This normalized quantity was
438 then used in all downstream analyses.

439 For analysis of fragment density across rRNA loci, one count was added for all positions between
440 and including the 5'- and 3'- ends of reads. To correct for variability in sequencing depth, counts
441 at each position were divided by a sample size factor. Briefly, counts recorded in each genomic
442 region were summed for all samples and then the geometric mean was taken across samples to
443 yield a reference sample. The size factor for a given sample was the median counts in all regions
444 after normalizing counts to the reference samples.

445 **Analysis of oligo depletion efficiency**

446 To quantify the efficiency of rRNA depletion, the sum of reads mapping to rRNA loci was divided
447 by the total number of mapped reads in each sample. To compare the reads mapping to individual
448 coding regions following rRNA depletion and/or antibiotic treatment (Figures 3A-C, S2A-F, and
449 S3A), coding regions were filtered for expression by RPKM, and then the correlation between
450 RPKM for individual coding regions was compared using the SciPy statistical functions package.
451 Outliers for the ratio of reads per coding region following Ribo-Zero versus DIY treatment (Figure
452 S2A) were identified by measuring the distance for all genes in Cartesian coordinates from the
453 log-log least squares fit for all regions above the expression threshold. Outliers were defined as

454 genes for which this ratio was less than or greater than two standard deviations from the mean line.
455 Outliers in Figure S2D were hand-picked.

456 **Acknowledgements**

457 The co-first authors discussed and mutually agreed on the author order. We thank I. Frumkin and
458 I. Nocedal for comments on the manuscript, D. Parker and M. Guzzo for reagents, and M. Guo for
459 helpful discussions. This work was funded by an NIH grant to M.T.L. (R01GM082899), who is
460 also an Investigator of the Howard Hughes Medical Institute. This work was also supported by
461 NSF predoctoral graduate research fellowships to P.H.C. and C.K.G.

462

463 **References**

- 464 1. Hör J, Gorski SA, Vogel J. 2018. Bacterial RNA Biology on a Genome Scale. *Mol Cell*
465 70:785–799.
- 466 2. Croucher NJ, Thomson NR. 2010. Studying bacterial transcriptomes using RNA-seq. *Curr*
467 *Opin Microbiol* 13:619–624.
- 468 3. Creecy JP, Conway T. 2015. Quantitative bacterial transcriptomics with RNA-seq. *Curr*
469 *Opin Microbiol* 23:133–140.
- 470 4. Podnar J, Deiderick H, Huerta G, Hunicke-Smith S. 2014. Next-generation sequencing
471 RNA-Seq library construction. *Curr Protoc Mol Biol* 1–19.
- 472 5. Nagalakshmi U, Wang Z, Waern K, Shou C, Raha D, Gerstein M, Snyder M. 2008. The
473 transcriptional landscape of the yeast genome defined by RNA sequencing. *Science* (80-)
474 320:1344–1349.
- 475 6. Mortazavi A, Williams BA, McCue K, Schaeffer L, Wold B. 2008. Mapping and
476 quantifying mammalian transcriptomes by RNA-Seq. *Nat Methods* 5:621–628.
- 477 7. Westermann AJ, Gorski SA, Vogel J. 2012. Dual RNA-seq of pathogen and host. *Nat Rev*
478 *Microbiol* 10:618–630.
- 479 8. Herbert ZT, Kershner JP, Butty VL, Thimmapuram J, Choudhari S, Alekseyev YO, Fan J,
480 Podnar JW, Wilcox E, Gipson J, Gillaspay A, Jepsen K, BonDurant SS, Morris K, Berkeley
481 M, LeClerc A, Simpson SD, Sommerville G, Grimmett L, Adams M, Levine SS. 2018.
482 Cross-site comparison of ribosomal depletion kits for Illumina RNAseq library
483 construction. *BMC Genomics* 19:1–10.
- 484 9. Stewart FJ, Ottesen EA, DeLong EF. 2010. Development and quantitative analyses of a
485 universal rRNA-subtraction protocol for microbial metatranscriptomics. *ISME J* 4:896–
486 907.
- 487 10. He S, Wurtzel O, Singh K, Froula JL, Yilmaz S, Tringe SG, Wang Z, Chen F, Lindquist
488 EA, Sorek R, Hugenholtz P. 2010. Validation of two ribosomal RNA removal methods for
489 microbial metatranscriptomics. *Nat Methods* 7:807–812.
- 490 11. Huang Y, Sheth RU, Kaufman A, Wang HH. 2019. Scalable and cost-effective

- 491 ribonuclease-based rRNA depletion for transcriptomics. *Nucleic Acids Res.*
- 492 12. Sugimoto N, Nakano S, Katoh M, Matsumura A, Nakamuta H, Ohmichi T, Yoneyama M,
493 Sasaki M. 1995. Thermodynamic Parameters To Predict Stability of RNA/DNA Hybrid
494 Duplexes. *Biochemistry* 34:11211–11216.
- 495 13. Culviner PH, Laub MT. 2018. Global Analysis of the *E. coli* Toxin MazF Reveals
496 Widespread Cleavage of mRNA and the Inhibition of rRNA Maturation and Ribosome
497 Biogenesis. *Mol Cell* 70:868-880.e10.
- 498
- 499

500 **Figure Legends**

501 **Figure 1. Oligonucleotide selection for 16S rRNA.**

502 (A) Alignment of 16S sequences from 8 bacterial species (Ec = *E. coli*; Pa = *P. aeruginosa*; Rp =
503 *R. parkeri*; Cc = *C. crescentus*; Bs = *B. subtilis*; Ms = *M. smegmatis*; Mtb = *M. tuberculosis*; Sa =
504 *S. aureus*). Alignment gaps are shown as red lines in the particular species of the gap. Regions
505 with a gap in any species are highlighted in pink; these regions were not considered when designing
506 oligos.

507 (B) The position, length, and minimum T_m of all oligos plotted against the 16S alignment after the
508 indicated number of optimization cycles (top). The information content at each nucleotide position
509 of aligned regions is also shown (bottom, points). To highlight conserved regions, a sliding average
510 information content is also plotted (bottom, line).

511 (C) Oligo T_m statistics after multiple cycles of the T_m optimization algorithm. For each oligo ($n =$
512 250), we calculated the minimum T_m across the 8 species considered and then plotted the mean of
513 this value across all oligos (black). The T_m cannot be accurately estimated for oligos with multiple
514 sequential mismatches; the number of oligos with an undefined T_m is also plotted (blue).

515 (D) Histograms of minimum T_m for oligos at the indicated number of optimization cycles. Data
516 were generated as in (C), but oligo T_m minima were used to generate histograms rather than taking
517 the mean across all oligos. Oligos with an undefined T_m were not included in the histograms.

518 (E) Distribution of T_m values for each 16S-targeting oligo ($n = 8$) for each individual species
519 indicated. The mean T_m of oligos for each species is also shown (red lines). Note that the same
520 oligos are used for each species, but because of 16S sequence variability, the T_m can vary, as
521 illustrated for one particular oligo (blue).

522 **Figure 2. rRNA depletion by oligonucleotide-based hybridization.**

523 (A) Cartoon of the rRNA depletion process.

524 (B) Polyacrylamide gel showing total RNA from *E. coli*, *B. subtilis*, and *C. crescentus* pre- and
525 post-rRNA depletion using indicated probe sets. The first lane is a ladder. Approximate positions
526 of abundant RNAs, including rRNAs, is indicated on the right. Note that a lower contrast is shown
527 for the top portion of the gel to resolve 16S and 23S bands.

528 (C) Fraction of total reads aligning to rRNA for rRNA-undepleted and -depleted samples of *E.*
529 *coli*, *B. subtilis*, and *C. crescentus* total RNA.

530 (D) Summed read counts across the *E. coli* 16S, 23S, and 5S rRNAs pre- (red) and post- (blue)
531 depletion. The positions of oligos used for depletion are shown below.

532 **Figure 3. Our rRNA depletion strategy performs comparably to Ribo-Zero for RNA-seq.**

533 (A) Scatterplot showing correlation between \log_2 fold changes for *E. coli* coding regions following
534 rifampicin treatment, comparing rRNA depletion via Ribo-Zero with our depletion strategy. Fold
535 changes were calculated as the ratio of RPKM between rifampicin treated and untreated samples.
536 All coding regions with at least 64 RPKM in both untreated samples ($n = 1294$) were considered
537 in the analysis.

538 (B) Scatterplot showing correlation between \log_2 fold changes for *E. coli* coding regions following
539 chloramphenicol treatment, comparing rRNA depletion via Ribo-Zero with our depletion strategy.
540 Fold changes were calculated as the ratio of RPKM between chloramphenicol-treated and
541 untreated samples. All coding regions with at least 64 RPKM in both untreated samples ($n = 1294$)
542 were considered in the analysis.

543 (C) Scatterplot showing correlation between read counts (RPKM) for *E. coli* coding regions treated
544 with Ribo-Zero and our do-it-yourself (DIY) depletion strategy. All coding regions with at least
545 64 RPKM in both samples ($n = 1294$) were considered in the analysis.

546

547 **Supplemental Figure Legends**

548 **Figure S1. Oligonucleotide selection for 23S rRNA**

549 (A) Alignments of all 23S sequences from 8 bacterial species (Ec = *E. coli*; Pa = *P. aeruginosa*;
550 Rp = *R. parkeri*; Cc = *C. crescentus*; Bs = *B. subtilis*; Ms = *M. smegmatis*; Mtb = *M. tuberculosis*;
551 Sa = *S. aureus*). Alignment gaps are shown as red lines in the particular species of the gap. Regions
552 with a gap in any species are highlighted in pink; these regions were not considered when designing
553 oligos.

554 (B) The position, length, and minimum T_m of all oligos plotted against the 23S alignment after the
555 indicated number of optimization cycles (top). The information content at each nucleotide position
556 of aligned regions is also shown (bottom, points). To highlight conserved regions, a sliding average
557 information content is also plotted (bottom, line).

558 (C) Oligo T_m statistics after multiple cycles of the T_m optimization algorithm. For each oligo ($n =$
559 500), we calculated the minimum T_m across the 8 species considered and then plotted the mean of
560 this value across all oligos (black). The T_m cannot be accurately estimated for oligos with multiple
561 sequential mismatches; the number of oligos with an undefined T_m is also plotted (blue).

562 (D) Histograms of minimum T_m for oligos at the indicated number of optimization cycles. Data
563 were generated as in (C), but oligo T_m minima were used to generate histograms rather than taking
564 the mean across all oligos. Oligos with undefined T_m were not included in the histograms.

565 (E) Distribution of T_m values for each 23S-targeting oligo ($n = 11$) for each individual species
566 indicated. The mean T_m of oligos for each species is also shown (red lines). Note that the same
567 oligos are used for each species, but because of 23S sequence variability, the T_m can vary, as
568 illustrated for one particular oligo (blue).

569 **Figure S2. Analysis of outliers in correlation between mRNA counts following Ribo-Zero and** 570 **DIY rRNA depletion.**

571 (A) Figure 3C, with all genes at least two standard deviations away from the least squares fit line
572 (red) indicated in black ($n = 69$).

573 (B) Figure 3A, with outliers identified in Figure S3A marked in black. For these outliers, the
574 correlation between \log_2 (rif+/negative control) for DIY depletion and Ribo-Zero treatment was
575 0.95, compared to 0.98 for all well-expressed coding regions.

576 (C) Figure 3B, with outliers identified in Figure S3A marked in black. For these outliers, the
577 correlation between \log_2 (chl+/negative control) for DIY depletion and Ribo-Zero treatment was
578 0.90, compared to 0.97 for all well-expressed coding regions.

579 (D) Figure 3C, with 11 highly-expressed genes more depleted in our method than in Ribo-Zero
580 indicated in black.

581 (E) Figure 3A, with outliers identified in Figure S3D marked in black. For these outliers, the
582 correlation between \log_2 (rif+/negative control) for DIY depletion and Ribo-Zero treatment was
583 0.96, compared to 0.98 for all well-expressed coding regions.

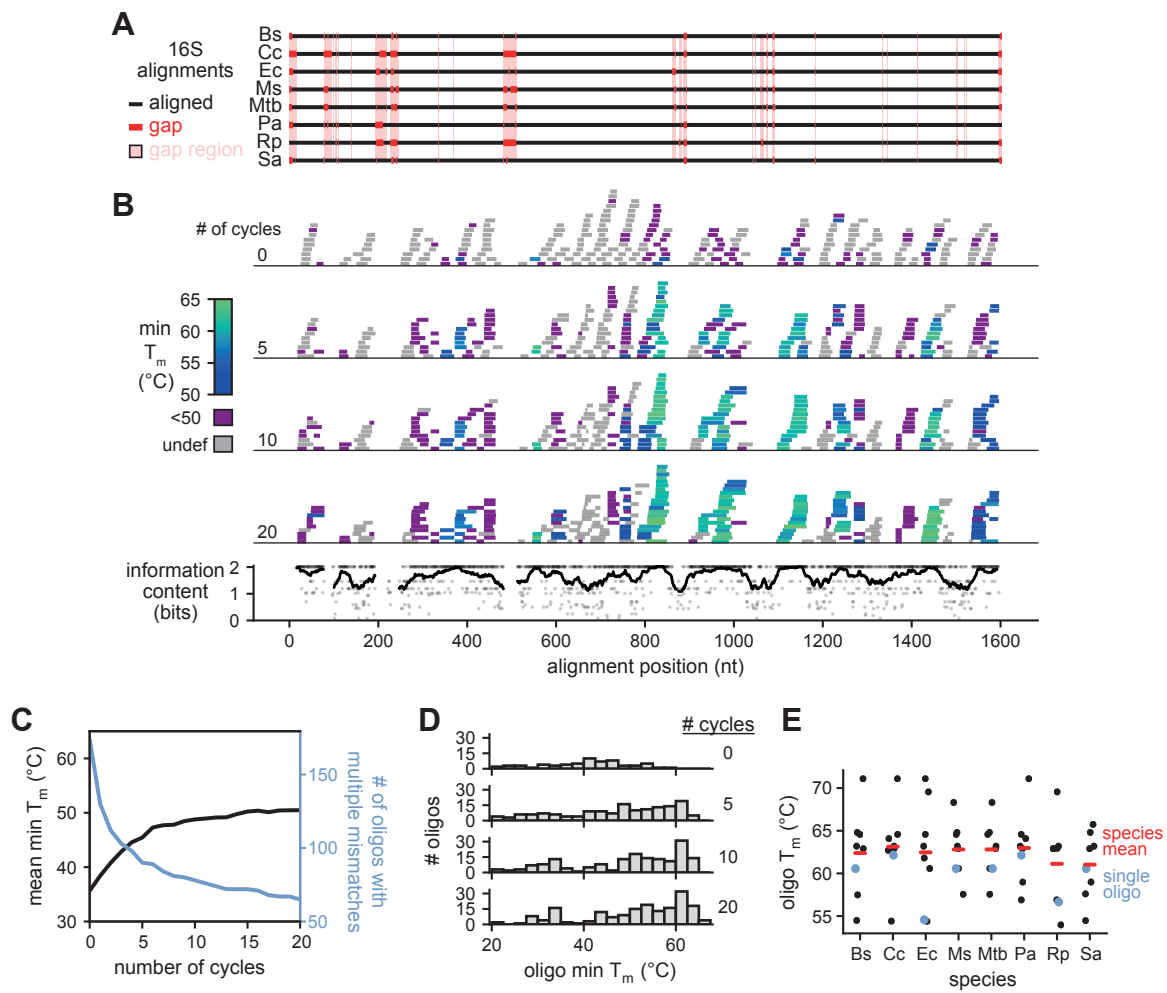
584 (F) Figure 3B, with outliers identified in Figure S3D marked in black. For these outliers, the
585 correlation between \log_2 (chl+/negative control) for DIY depletion and Ribo-Zero treatment was
586 0.89, compared to 0.97 for all well-expressed coding regions.

587 **Figure S3. Correlation between counts per coding region pre- and post-rRNA depletion for**
588 ***B. subtilis* and *C. crescentus* total RNA.**

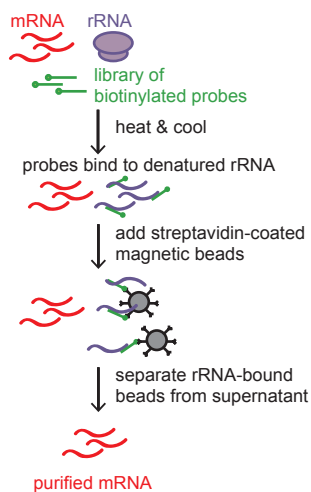
589 (A) Top left: scatterplot showing correlation between read counts (RPKM) for *E. coli* coding
590 regions pre- and post-rRNA depletion using our depletion strategy. All coding regions with at least
591 10 counts in both samples ($n = 438$) were considered in this analysis. Top right: scatterplot showing
592 correlation between read counts (RPKM) for *B. subtilis* coding regions pre- and post-rRNA
593 depletion using our depletion strategy. All coding regions with at least 10 counts in both samples
594 (784 regions total) were considered in the analysis. Bottom: scatterplot showing correlation
595 between read counts (RPKM) for *C. crescentus* coding regions pre- and post-rRNA depletion using
596 our depletion strategy. All coding regions with at least 10 counts in both samples (398 regions
597 total) were considered in the analysis.

598 (B) Fold-depletion for various ratios of oligo probe : RNA and streptavidin bead : oligo probe
599 ratios. Depletions were calculated by qRT-PCR to a single region within each rRNA relative to a
600 bead-only negative control.

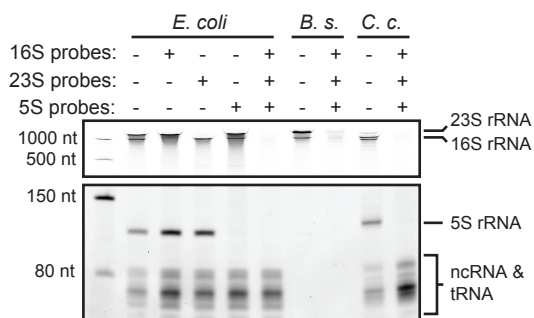
Figure 1



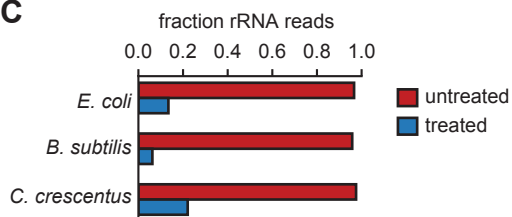
A



B



C



D

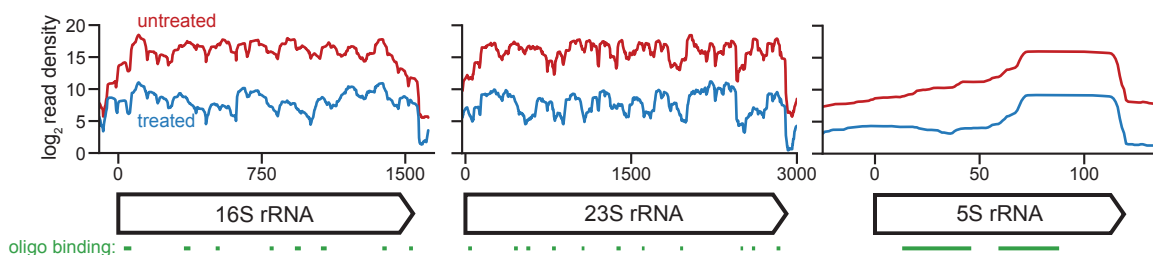
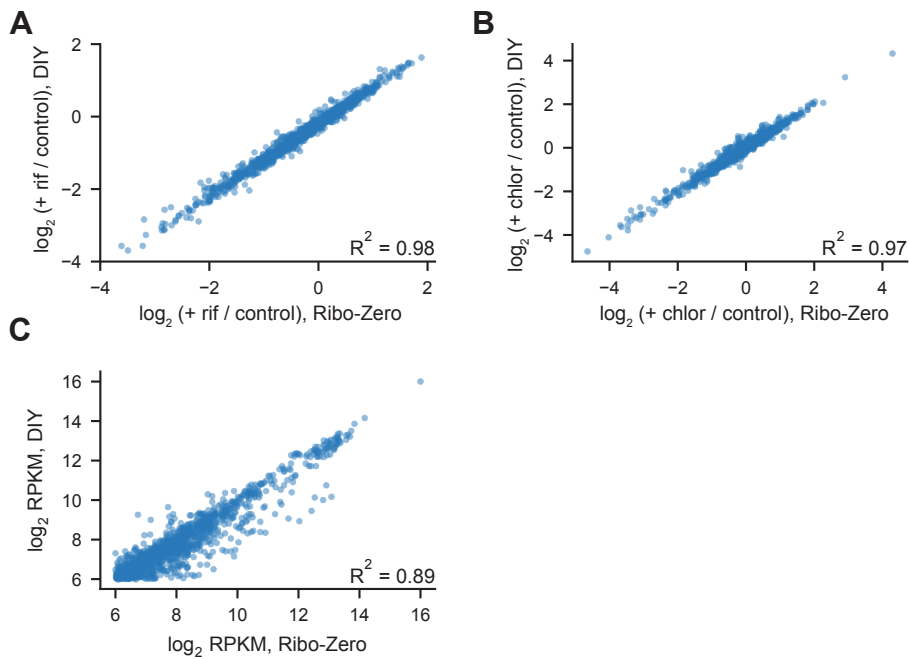
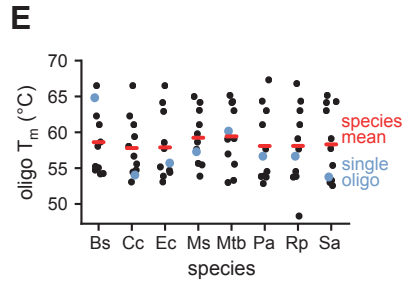
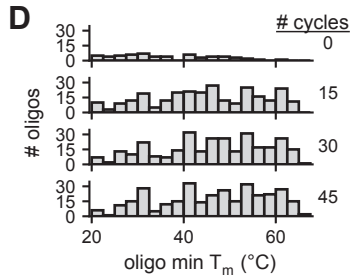
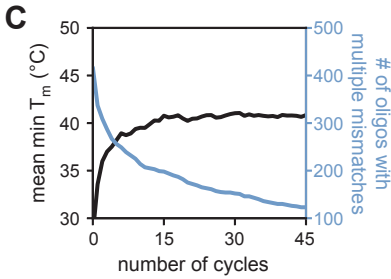
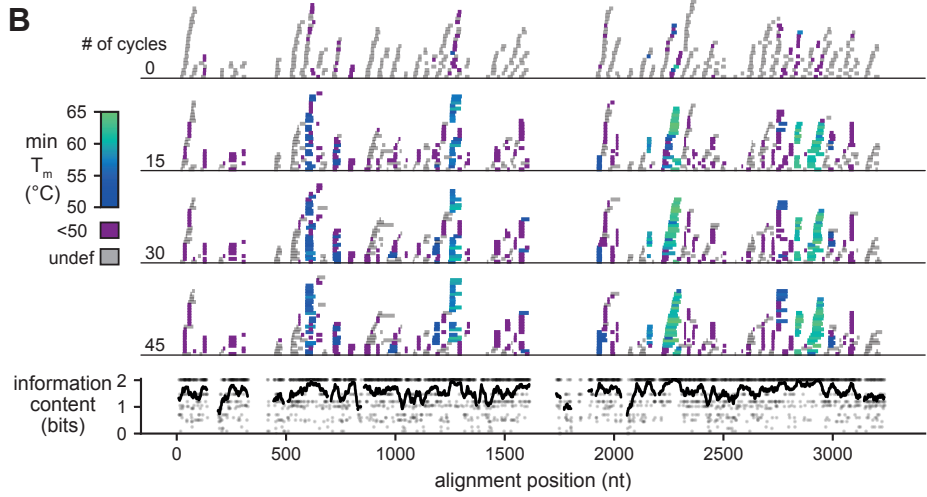
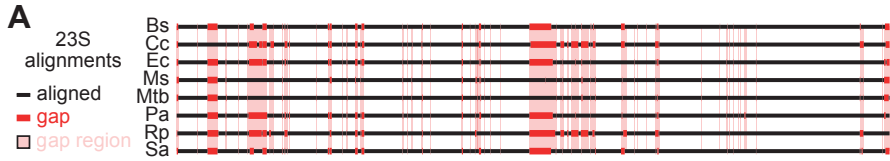
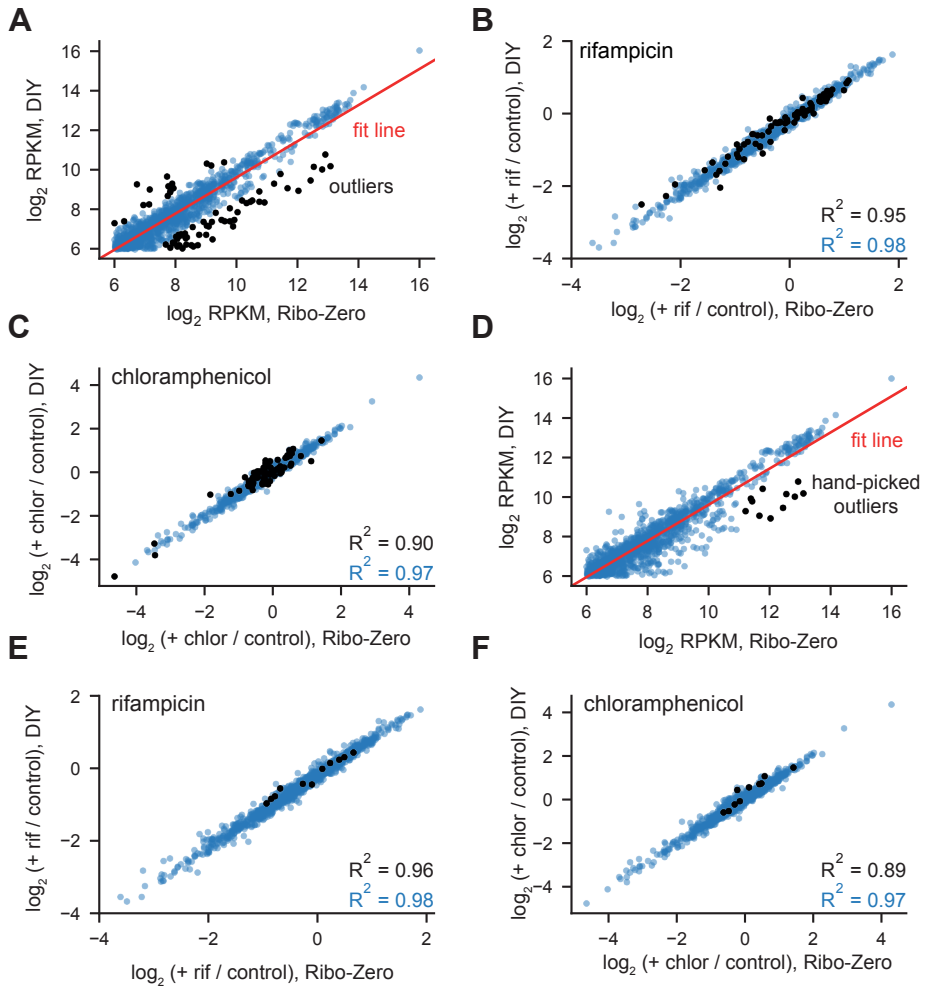


Figure 3







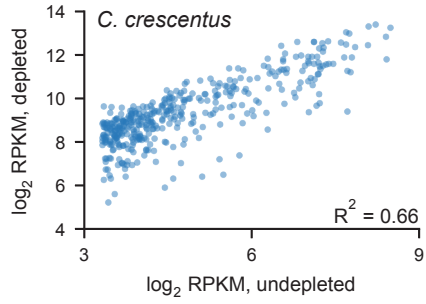
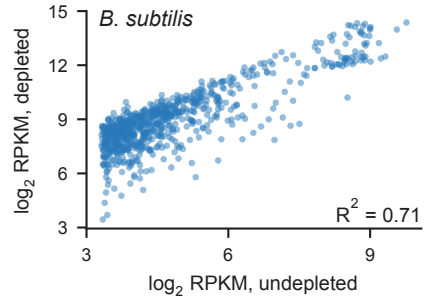
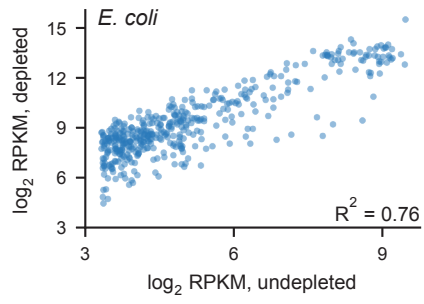
A

Table S1 - Sequences of oligonucleotides for bacterial rRNA depletion

<u>Name</u>	<u>Sequence</u>
23S_1	ACCTTTCCCTCACGGTACTGGTTCGCTATCGGTCA
23S_2	AGTCGCTGGCTCATTATACAAAAGGTACGCCGTCACC
23S_3	TCGGGGAGAACCAGCTATCTCCGGGTTTGATTGGC
23S_4	GTGGCTGCTTCTAAGCCAACATCCTG
23S_5	GGGTACAGGAATATTAACCTGATTTCCATCGACTACGCC
23S_6	CACCTGTGTCGGTTTGGGGTACGGT
23S_7	TCGTGCGGGTCGGAACCTTACCCGACAAG
23S_8	GAGCCGACATCGAGGTGCCAAACA
23S_9	CGGCGGATAGGGACCGAACTGTCTCACGAC
16S_1	CCGCTCGACTTGCATGTGTTAAGCATGCCGACAGCGTTCC
16S_2	CCCATTGTGCAAGATTCCCTACTGCTGCCTCCCGT
16S_3	ACCGCGGCTGCTGGCACGGAGT
16S_4	ACGGCGTGGACTACCAGGGTAT
16S_5	TCCACATGCTCCACCGCTTGTGCGGGCCCCCG
16S_6	ACCCAACATCTCACAAACACGAGCTGACGACA
16S_7	GGGCAGTGTGTACAAGGCCCGGGA
16S_8	AAGGAGGTGATCCAGCCGCAG
23S_GN1	CACGTCCTTCATCGCCTTTTACTGCCAAGGCATCC
23S_GN2	CCACACCCGGCCTATCAACGTGGTGGTCTTCGACG
23S_GP1	ATGCCAAGGCATCCACCATGCGCCCT
23S_GP2	TATCCTGTCCGCACGTGGCTACCCAGCG
5S_EcPa_1	GTTTCGGGAAGGGGTTCAGGTGGGTCCAACGCGCTA
5S_EcPa_2	AGACCCACACTACCATCGGCGATACGTCG
5S_Sa_1	GCATGGGAACAGGTGTGACCTCCTTGCTAT
5S_Sa_2	GCGGAACGTAAGTTCGACTACCATCGACGCT
5S_Bs_1	GGTATGGGAACGGGTGTGACCTCTTCGCTA
5S_Bs_2	CGACTACCATCGGCGCTGAAGAGCTTAAC
5S_Cc_1	CCGAGTTCGGAATGGGATCGGGTGGG
5S_Cc_2	CTTGAGACGAAGTACCATTGGCCCAGGG
5S_Rp_1	GGATGGGATCGTGTGTTTCACTCATGCTATAACCACC
5S_Rp_2	TCCCATGCCTTATGACATAGTACCATTAGCGCTAT
5S_MtbMs_1	ACCGGGCGTTTCCCTGCCGCTA
5S_MtbMs_2	GGTAGTATCATCGGCGCTGGCAGG